FEMS Yeast Research, 2025, **25**, foaf015
DOI: 10.1093/femsyr/foaf015
Advance access publication date: 29 March 2025
Research Article – Genetics, cell biology and metabolism

The physiology of an engineered *Saccharomyces cerevisiae* strain that carries both an improved glycerol-3-phosphate and the synthetic dihydroxyacetone pathway for glycerol utilization

Andreea Perpelea[1,‡], Frederico Mendonça Bahia[1,2,‡], Joeline Xiberras[1,3], Putu Virgina Partha Devanthi[1,4], Paola Branduardi[2], Mathias Klein[1], Elke Nevoigt[1,*]

[1]School of Science, Constructor University, 28759 Bremen, Germany
[2]Department of Biotechnology and Biosciences, University of Milano Bicocca, 20126 Milan, Italy
[3]Present address: RGR/D White Biotechnology Research, BASF SE, 67056 Ludwigshafen am Rhein, Germany
[4]Department of Biotechnology, School of Life Sciences, Indonesia International Institute for Life Sciences, 13210 Jakarta, Indonesia
*Corresponding author. School of Science, Constructor University, Campus Ring 1, 28759 Bremen, Germany. E-mail: enevoigt@constructor.university
Editor: [Hyun Ah Kang]
‡These authors equally contributed to the work.

Abstract

Our laboratory previously established variants of the *Saccharomyces cerevisiae* strain CEN.PK113-1A able to grow in synthetic glycerol medium. One approach focused on improving the endogenous l-glycerol-3-phosphate (G3P) pathway, while a second approach aimed to replace the endogenous pathway with the dihydroxyacetone (DHA) pathway. The latter approach led to a significantly higher maximum specific growth rate (μ_{max}) of 0.26 h^{-1} compared to 0.14 h^{-1}. The current study focused on combining all genetic modifications in one strain. Apart from the so-called "TWO pathway strain" (CEN TWO_{PW}), two isogenic control strains, CEN $G3P_{PW}$ and CEN DHA_{PW}, were constructed. The μ_{max} of CEN TWO_{PW} (~0.24 h^{-1}) was virtually identical to that of CEN DHA_{PW}. Remarkable characteristics of the strain CEN TWO_{PW} compared to CEN DHA_{PW} include a higher specific glycerol consumption rate, the capacity to deplete glycerol completely, and a much higher ethanol and lower biomass formation during oxygen-limited shake flask cultivations. The results obtained with different alleles of the *GUT1* gene, encoding for glycerol kinase, suggest that the phenotype of the strain CEN TWO_{PW} is at least partly attributed to the particular point mutation in the *GUT1* allele used from the strain JL1, which was previously generated through adaptive laboratory evolution.

Keywords: baker's yeast; metabolic engineering; glycerol; G3P pathway; DHA pathway; GUT1

Introduction

Glycerol offers several advantages as a feedstock for industrial biotechnology when compared to sugars. First, its liquid form minimizes dilution effects even when feeding at high concentrations throughout fermentation. Second, its higher degree of reduction per carbon atom allows for higher maximum theoretical yields of target molecules whose formation requires additional electrons (Clomburg and Gonzalez 2013). Moreover, glycerol enables electron-neutral co-fermentation of oxidized substrates, e.g. carbon dioxide (Steiger et al. 2017) and galacturonic acid (Perpelea et al. 2022).

Glycerol is an agricultural by-product mainly generated in oil-plant biorefineries and in the biodiesel, oleochemical, and bioethanol industries (Russmayer et al. 2019). The available glycerol has mainly been generated due to the growth of the biodiesel industry (Yang et al. 2012). The potential application of engineered microorganisms for lipid production in the biodiesel industry could offer even more sustainable sources of glycerol in the future (Hu et al. 2016). The latter is particularly interesting if gas mixtures of CO, CO_2, and H_2 are used as microbial substrates (Takors et al. 2018).

Glycerol can naturally be used by many yeast species as the sole source of carbon and energy (Kurtzman et al. 2011). However, most strains of *Saccharomyces cerevisiae* are either unable to grow in synthetic glycerol medium (SMG) or show a relatively low maximum specific growth rate (μ_{max}) (Swinnen et al. 2013, Ho et al. 2017). Nevertheless, our laboratory has successfully overcome the complete inability of the popular laboratory *S. cerevisiae* strain CEN.PK113-1A to utilize glycerol in synthetic medium. Different strain variants have been constructed, which can be grouped into two major classes. One group exclusively contains modifications of endogenous genes, leading to glycerol metabolism via the endogenous flavin adenine dinucleotide (FAD)-dependent L-glycerol-3-phosphate pathway ("G3P pathway"). The second group was constructed under the premise of making glycerol utilization nicotinamide adenine dinucleotide (NAD)-dependent via an alternative pathway, the dihydroxyacetone (DHA) pathway, by expressing a heterologous glycerol dehydrogenase, increasing the activity

Received 29 August 2024; **revised** 4 March 2025; **accepted** 28 March 2025

of the endogenous DHA kinase, and abolishing the endogenous G3P pathway. Notably, the DHA pathway approach resulted in significantly higher specific growth rates. The best-performing variants of each approach are shown in Fig. 1A and B. The following paragraphs provide more details about the genetic modifications and strain construction history since they are relevant for the current study.

Wild-type *S. cerevisiae* strains contain the genes required for the L-glycerol-3-phosphate (L-G3P) pathway. Glycerol uptake is mediated by a glycerol/H^+ symporter encoded by *STL1* (Ferreira et al. 2005), and glycerol is phosphorylated by an ATP-dependent glycerol kinase encoded by *GUT1* (Sprague and Cronan 1977, Pavlik et al. 1993). The resulting L-G3P is then oxidized by an FAD-dependent glycerol dehydrogenase encoded by *GUT2* (Sprague and Cronan 1977, Rønnow and Kielland-Brandt 1993) to the glycolytic intermediate dihydroxyacetone phosphate (DHAP). Gut2 is located at the outer surface of the inner mitochondrial membrane, channeling the electrons via $FADH_2$ to the ubiquinone pool of the respiratory chain. Despite having the genes for the "G3P pathway", many common laboratory wild-type *S. cerevisiae* strains (including the CEN.PK family) do not grow at all when glycerol is the sole source of carbon in synthetic medium in which amino acid/nucleic base supplements are omitted (Swinnen et al. 2013). However, the same study revealed a few natural *S. cerevisiae* isolates, including the strain CBS 6412, that can grow under these conditions. Therefore, one route toward an improved variant of the strain CEN.PK113-1A was to unravel the crucial genetic determinants for the superior growth phenotype of the strain CBS 6412, more precisely the haploid segregant CBS 6412-13A. Successful quantitative trait loci (QTL) mapping and allele replacement identified superior mutations in *GUT1* and *UBR2*, and the respective alleles were referred to as $GUT1_{CBS}$ and $UBR2_{CBS}$ (Swinnen et al. 2016). The *UBR2* gene encodes a ubiquitin ligase functioning in the ubiquitin proteasome system of *S. cerevisiae* (Finley et al. 2012), but its relevance for glycerol utilization has remained unclear. The relevance of the $GUT1_{CBS}$ and $UBR2_{CBS}$ resulted in growth on glycerol in synthetic medium.

In parallel, adaptive laboratory evolution (ALE) was used to obtain CEN.PK113-1A variants that can grow in SMG as shown by Ochoa-Estopier et al. (2011). We analyzed the evolved strain JL1 by whole-genome sequencing. Interestingly, the data revealed single nucleotide polymorphisms in *GUT1* and *UBR2*, although the SNPs were different from those in CBS 6412-13A (Swinnen et al. 2016). The alleles have been referred to as $GUT1_{JL1}$ and $UBR2_{JL1}$, and the combination of the two allele replacements in the CEN.PK113-1A background resulted in a maximum specific growth rate of 0.13 h^{-1}. Ho et al. (2017) also tested combinations between the superior alleles obtained from CBS 6412-13A and JL1. The best-performing strain, showing a slightly higher μ_{max} of 0.14 h^1, has been named CEN.PK113-1A $UBR2_{CBS}$ $GUT1_{JL1}$ (Fig. 1A). It is worth noting that the coding sequence of $GUT1_{CBS}$ carries multiple amino-acid exchanges compared to the wild-type *GUT1* allele from CEN.PK113-1A, while the coding sequence of $GUT1_{JL1}$ only carries a single mutation (Ser118Phe), which is different from the mutations detected in $GUT1_{CBS}$ (Ho et al. 2018).

This paragraph will summarize our achievements when using the second approach, i.e. establishing the synthetic DHA pathway as the sole glycerol catabolic pathway in CEN.PK113-1A. This approach included the heterologous expression of *Ogataea parapolymorpha*'s glycerol dehydrogenase (*Opgdh*) previously characterized by Yamada-Onodera et al. (2002) and the overexpression of an endogenous dihydroxyacetone kinase ($DAK1_{oe}$). Additionally, we expressed a heterologous aquaglyceroporin (Fps1 homolog) from *Cyberlindnera jadinii (CjFPS1)*, motivated by our previous finding that the individual expression of aquaglyceroporins from various non-*S. cerevisiae* yeast species significantly improved the growth of the strain CBS 6412-13A in SMG (Klein et al. 2016b). All expression cassettes were integrated in the *GUT1* locus, thereby abolishing the metabolic flux through the endogenous G3P pathway and forcing glycerol catabolism via the DHA pathway, which generates NADH (reduced form of NAD) (Fig. 1B). The highest μ_{max} achieved with this approach in SMG has been 0.26 h^{-1}. As a side note, our lab constructed several DHA pathway strains, only varying in the number of *DAK1* expression cassettes, promoters, and genomic integration sites. The μ_{max} of all "DHA pathway strains" on glycerol differed only slightly from the rate measured with the strain originally constructed by Klein et al. (2016a).

With regard to improving the utilization of glycerol of the strain CEN.PK113-1A, there still remained the unanswered question of whether the simultaneous presence of the established DHA pathway and the improved endogenous G3P pathway could bring about additional advantages over strains that only exhibit the DHA pathway. In fact, bioprocesses would profit from a higher μ_{max} and/or glycerol consumption rate. The current study therefore aimed at constructing a "TWO pathway strain" in the CEN.PK background by combining all genetic modifications that were previously used in the two approaches to separately optimize the G3P and the DHA pathways. Figure 1C shows the constitution of the strain CEN TWO_{PW} as well as two newly constructed reference strains, CEN $G3P_{PW}$ and CEN DHA_{PW}, which only differ in the pathways from glycerol to DHA but are otherwise isogenic to the strain CEN TWO_{PW}.

Methods

Strains and plasmids

All *S. cerevisiae* strains used and constructed in this study are listed in Supplementary Table S1. Yeast cells were routinely grown at 30°C on solid (static incubator) or in liquid (orbital shaking incubator, 200 rpm) yeast extract peptone dextrose (YPD) medium containing 10 g/l yeast extract, 20 g/l peptone, and 20 g/l glucose (with the addition of 15 g/l agar for solid medium). When needed, phleomycin (20 mg/l), nourseothricin (100 mg/l), or hygromycin B (300 mg/l) was added to the medium for selection purposes.

Escherichia coli DH5α was used for plasmid maintenance, propagation, and isolation. All plasmids used (and constructed) in this study are listed in Supplementary Table S2. Bacterial cells were routinely grown at 37°C on solid (static incubator) or in liquid (orbital shaking incubator, 250 rpm) lysogeny broth (LB) containing 5 g/l yeast extract, 10 g/l peptone, and 10 g/l NaCl, pH 7.5 (with the addition of 15 g/l agar for solid medium). Plasmids were maintained by the addition of 100 mg/l ampicillin to the medium.

General molecular biology techniques

Polymerase chain reaction (PCR) was performed either with Phusion® High-Fidelity DNA Polymerase (when PCR products were used for cloning and sequencing) or OneTaq® QuickLoad® DNA Polymerase (for diagnostic PCR), both from New England Biolabs (Ipswich, MA, USA). All primers used in this study for strain construction are listed in Supplementary Table S3. The primers used for plasmid construction are shown in Supplementary Table S4. PCR was carried out following the manufacturer's guidelines. Plasmids were isolated from *E. coli* with the GeneJET Plasmid Miniprep Kit (Thermo Fisher Scientific Inc., Waltham, MA, USA) following the manufacturer's protocol. PCR products were purified using the

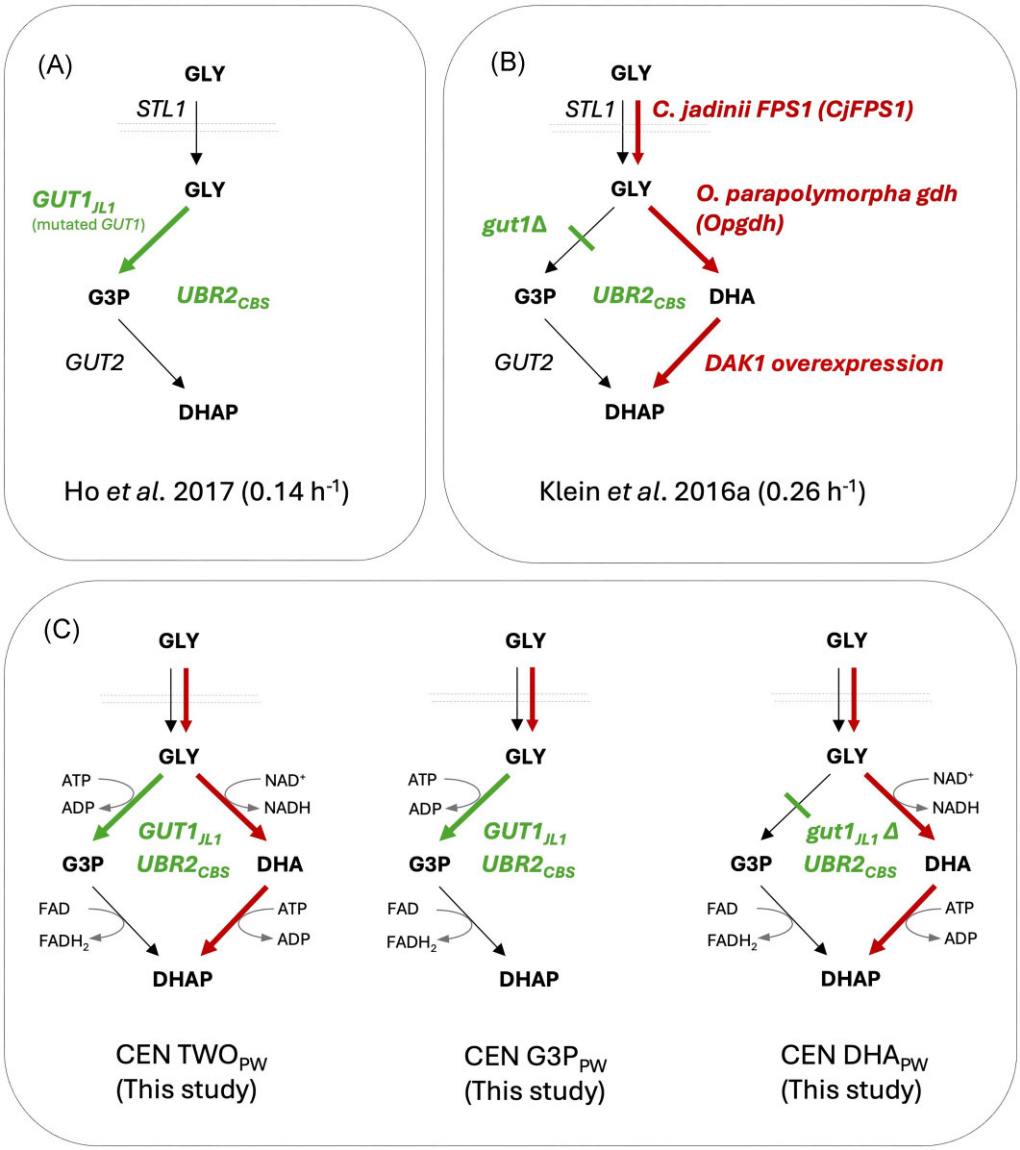

Figure 1. Engineering of *S. cerevisiae* for improved utilization of glycerol via the G3P and/or the DHA pathway. While the genetically modified derivatives of the CEN.PK113-1A strain background shown in (A) and (B) have been previously published, the CEN TWO_{PW} strain (which allows glycerol catabolism via both pathways) and the two isogenic reference strains, CEN $G3P_{PW}$ and CEN DHAPW shown in (C), have been constructed in the current study. The difference of the latter two and the previously published strains regards the used promoters driving expression and the used integration sites. Genetic modifications that led to the best-performing strain on glycerol based on the G3P pathway are shown in green. Transport and enzymatic reactions that have previously been engineered to construct the best-performing DHA pathway strain are shown in red. GLY, glycerol; DHA, dihydroxyacetone; G3P, L-glycerol-3-phosphate; DHAP, dihydroxyacetone phosphate; *STL1*, glycerol/H^+ symporter; *GUT1*, glycerol kinase—the $GUT1_{JL1}$ allele was derived from the evolved, glycerol-growing strain JL1 as described by Ho et al. (2017); *GUT2*, mitochondrial FAD-dependent L-glycerol-3-phosphate dehydrogenase; *CjFPS1*, aquaglyceroporin ("glycerol facilitator"); *Opgdh*, NAD-dependent glycerol dehydrogenase; *DAK1/2*, endogenous dihydroxyacetone kinase; *UBR2*, ubiquitin ligase functioning in the ubiquitin proteasome system—the $UBR2_{CBS}$ allele was derived from the strain CBS 6412-13A and used to replace the endogenous *UBR2* allele of strain CEN.PK113-13A as described by Ho et al. (2017).

GeneJET PCR Purification Kit (Thermo Fisher Scientific Inc.) according to the manufacturer's instructions. Transformation of *S. cerevisiae* with plasmids as well as linear DNA fragments for genomic integration was performed according to the previously described lithium acetate method (Gietz and Schiestl 2007).

Strain construction

Strains CEN $G3P_{PW}$, CEN DHA_{PW}, and CEN TWO_{PW}

Supplementary Fig. S1 depicts the process of constructing the strains CEN $G3P_{PW}$, CEN DHA_{PW}, and CEN TWO_{PW}. The construction of the strains CEN DHA_{PW} and CEN TWO_{PW} has already been described in Malubhoy et al. (2022) in which the strain CEN DHA_{PW} served as a baseline for establishing SA production. The strain CEN DHA_{PW} was simply obtained by deleting $GUT1_{JL1}$ in strain CEN TWO_{PW}. In the study of Malubhoy et al. (2022), the strain CEN TWO_{PW} was called $UBR2_{CBS}$-$GUT1_{JL1}$-DHA, while CEN DHA_{PW} was called $UBR2_{CBS}$-DHA (2). In order to better understand the construction history of the three strains mentioned as relevant in the current study, a short description is included here as well. The strain CEN.PK113-1A $UBR2_{CBS}$ $GUT1_{JL1}$ (Supplementary Table S1) served as a starting point in which the expression cassettes for *CjFPS1*, *Opgdh*, and *DAK1* were integrated at the *YGLCτ3* genomic locus via CRISPR/Cas9-mediated genomic integration. The

YGLCτ3 locus has been described by Bai Flagfeldt et al. (2009). The above strain was first transformed with the plasmid p414-TEF1p-Cas9-CYC1t-natMX. The Cas9-expressing strain was then co-transformed with the plasmid p426-SNR52p-gRNA.YGLCτ3-target-SUP4t-hphMX (for gRNA expression) and the respective repair fragments for assembly and integration at the *YGLCτ3* locus as shown in Supplementary Fig. S1. The fragments to be assembled and integrated were obtained by PCR using primers carrying 5′-extensions that generated regions of 52–81 bp homology either to the adjacent fragments or to the genomic sequences upstream and downstream of the double-strand break inserted by Cas9. All used primer sequences, the respective amplified DNA fragments, and the used templates are shown in Supplementary Table S3. The *TDH3* promoter (used for the assembly of the *CjFPS1* expression cassette) and the *ADH2* promoter (used for the assembly of the *DAK1* expression cassette) were both amplified from genomic DNA isolated from the strain CEN.PK113-7D $UBR2_{JL1}$ $GUT1_{JL1}$ (Supplementary Table S1). All other fragments were amplified from the plasmids shown in Supplementary Table S2. Positive transformants were selected on YPD agar containing both nourseothricin and hygromycin B. The resulting strain only carrying the *CjFPS1* cassette in the *YGLCτ3* locus was named CEN $G3P_{PW}$, while the strain additionally carrying the cassettes for the expression of *Opgdh* and *DAK1* was named CEN TWO_{PW}. Following the confirmation of transformants, both Cas9 and gRNA-containing plasmids were removed via serial cultivations in YPD medium without any antibiotic. The strain CEN DHA_{PW} was then constructed by deleting $GUT1_{JL1}$ in the strain CEN TWO_{PW} by integrating the *ble* cassette for phleomycin resistance (Supplementary Fig. S1).

Strain CEN TWO_{PW} gut2Δ

Alternative to deleting *GUT1* for abolishing the flux via the L-G3P pathway (CEN TWO_{PW} $gut1_{JL1}$Δ corresponding to strain CEN DHA_{PW}), a strain was constructed in which *GUT2* was deleted and is referred to here as CEN TWO_{PW} *gut2*Δ. In analogy to the deletion of *GUT1*, *GUT2* was deleted using the *ble* cassette amplified from plasmid pUG66 (Supplementary Table S2) and the respective primers as shown in Supplementary Table S3.

Strain CEN TWO_{PW} carrying different alleles of GUT1

In order to obtain CEN TWO_{PW} variants carrying different alleles of *GUT1*, the *ble* resistance cassette in strain CEN DHA_{PW} was replaced by the respective coding sequences using CRISPR/Cas9-mediated genome editing. Initially, a plasmid for the expression of a gRNA targeting the *ble* disruption cassette was constructed. For this purpose, the 20 nt sequence in p426-SNR52pgRNA.CAN1. Y-SUP4t-hphMX (Supplementary Table S2) targeting the *CAN1* gene was replaced by 20 nt targeting the *ble* resistance marker. The target sequence within the *ble* coding sequence was selected using the CRISPRdirect online tool developed by Naito et al. (2015). First, two overlapping PCR products of the gRNA expression cassette were generated using p426-SNR52p-gRNA.CAN1. Y-SUP4t-hphMX as a template and the primers shown in Supplementary Table S4. The vector was cleaved using *Pvu*II to remove the original gRNA expression cassette, and the vector backbone was subsequently purified from an agarose gel. The overlapping PCR fragments and the purified vector backbone were subsequently assembled according to Gibson et al. (2009). The one-step isothermal DNA assembly reaction was prepared as described by Gibson et al. (2009), containing 15 μl of the reagent-enzyme mix, 0.05 pmol of *Pvu*II-linearized vector, and three-fold molar excess of the inserts (each 0.15 pmol) in a final volume of 20 μl. The reaction mixture was incubated at 50°C for 1 h. *Escherichia coli* DH5α cells were transformed with 5 μl of the reaction. The resulting vector was named p426-SNR52p-gRNA.ble-SUP4t-hphMX.

For replacement of the *ble* resistance marker by the different *GUT1* alleles (i.e. different coding sequences), the strain CEN DHA_{PW} was first transformed with p414-TEF1p-Cas9-CYC1t-natMX. The $GUT1_{CBS}$ coding sequence was amplified from genomic DNA isolated from CBS 6412-13A, and the $GUT1_{JL1}$ coding sequence was amplified from strain CEN.PK113-1A $UBR2_{JL1}$ $GUT1_{JL1}$. The used primers (Supplementary Table S3) contained 5′-extensions generating 40–60 bp sequences homologous to regions directly upstream and downstream of the inserted *ble* resistance marker. The hybrid variant ($GUT1_{hybrid}$) combining the single point mutations from both $GUT1_{CBS}$ and $GUT1_{JL1}$ was obtained by generating two overlapping PCR products using genomic DNA from CBS 6412-13A as a template. The used primers were designed in a way that the overlap of the two PCR products contained the nucleotide exchange, introducing the single point mutation from $GUT1_{JL1}$ into the coding sequence after assembly and integration at the *GUT1* locus and replacing the *ble* resistance marker (Supplementary Fig. S2). The Cas9-expressing CEN DHA_{PW} strain was co-transformed with p426-SNR52p-gRNA.ble-SUP4t-hphMX for gRNA expression and the fragments of the *GUT1* coding sequences, resulting in assembly and integration at the target locus, replacing the *ble* resistance marker, and restoring the *GUT1* gene. Positive transformants were selected on YPD agar containing both nourseothricin and hygromycin B. Both vectors were subsequently removed from the resulting clones by serial transfers in YPD medium lacking the respective antibiotics.

Verification of genomic modifications

All modifications of chromosomal DNA were verified by isolating genomic DNA followed by diagnostic PCR. Yeast genomic DNA was isolated using PCI (phenol-chloroform-isoamyl alcohol mixed in a ratio of 25:24:1) according to the protocol from Hoffman and Winston (1987), which was slightly modified. Approximately 50 mg of cells (wet weight) were resuspended in 200 µl of TE buffer (10 mM Tris, 1 mM EDTA, pH 8) together with 0.3 g of acid-washed beads (0.425–0.6 mm). To this mixture, 200 µl of PCI were added, and the tubes were vortexed at maximum speed for 2 min. The tubes were centrifuged at 15,700 *g* for 10 min, and the upper phase containing the genomic DNA was directly used for diagnostic PCR. Specifically, 1 µl of a 1:20 dilution (in ddH_2O), served as a template for a PCR of a total volume of 25 µl. Primers were designed where one binds outside the integration locus and the other one within the integrated fragments. When several fragments were integrated, primers were also designed to amplify across the junctions between the integrated fragments. The relevant genetic modifications in all new constructs were also confirmed using Sanger sequencing.

Media and growth conditions

All experiments conducted for the physiological characterization of the constructed *S. cerevisiae* strains were performed in synthetic medium prepared according to Verduyn et al. (1992). However, there have been variations with regards to the carbon source, the nitrogen source, and the pH as indicated. Synthetic medium with glucose as a carbon source and ammonium sulfate as a nitrogen source (SMD) contained per liter: 5 g $(NH_4)_2SO_4$, 3 g KH_2PO_4, 0.5 g $MgSO_4{\cdot}7H_2O$, 15 mg EDTA, 4.5 mg $ZnSO_4{\cdot}7H_2O$, 0.84 mg $MnCl_2{\cdot}2H_2O$, 0.3 mg $CoCl_2{\cdot}6H_2O$, 0.3 mg $CuSO_4{\cdot}5H_2O$, 0.4 mg $NaMoO_4{\cdot}2H_2O$, 4.5 mg $CaCl_2{\cdot}2H_2O$, 3 mg $FeSO_4{\cdot}7H_2O$, 1 mg

H_3BO_3, and 0.1 mg KI. The pH of the resulting solution was set to 6.5 using 4 M KOH. After heat sterilization, stock solutions for glucose and vitamins were added, resulting in final concentrations of 20 g/l for glucose and 0.05 mg/l D-(+)-biotin, 1 mg/l D-pantothenic acid hemicalcium salt, 1 mg/l nicotinic acid, 25 mg/myo-inositol, 1 mg/l thiamine chloride hydrochloride, 1 mg/l pyridoxine hydrochloride, and 0.2 mg/l 4-aminobenzoic acid. Synthetic medium with glycerol (7.5% w/v pure glycerol) contained 2.27 g/l of urea (SMG) as the sole nitrogen source. The pH of glycerol-containing media was set to either 4 or 5 using 2 M H_3PO_4 or 4 M KOH, respectively.

Determination of maximum specific growth rates was carried out by growing the strains in the Growth Profiler CR9001 (Enzyscreen, Haarlem, The Netherlands) using a protocol adapted from Swinnen et al. (2013). Single colonies were used to inoculate 3 ml SMD in 10 ml glass tubes. The tubes were placed at an incline (30°) into an orbital shaker, and cells were grown at 200 rpm and 30°C overnight. A 4 ml intermediate culture in SMD was inoculated to an initial OD_{600} of 0.2 and cultivated for 24 h under the same conditions. Of the resulting culture, 1 ml was harvested and washed once in the main culture medium (SMG, pH 5). One washing step consisted of centrifuging 1 ml of culture (854 × *g* for 5 min), removing the supernatant, and resuspending the cells in an equivalent volume of main culture medium. After an additional centrifugation step (854 × *g* for 7 min), the washed cells were resuspended in 1 ml SMG, and an appropriate amount was used to inoculate a 4 ml main culture to an OD_{600} of 0.2. From this culture, two 750 µl aliquots were transferred into 24-well plates (White Krystal 24-Well clear bottom microplate, Porvair Sciences, Leatherhead, UK) and allowed to grow in the Growth Profiler at 30°C and 200 rpm, where the plates were scanned at 30-min intervals. The Green Values (G-value) automatically extracted from the scans were correlated to OD_{600} values (Analytik Jena SPECORD 200 UV/VIS spectrophotometer) using the calibration curve below.

$$OD_{600} = 0.0144926245902538 \times G - value + 0.000148778009435622 \times G - value^{2.17758952130659}$$

Pre- and intermediate cultures for the experiments conducted in shake flasks followed the precultivation strategy described for the Growth Profiler, with the mention that the volumes of the pre- and intermediate cultures were increased to 5 and 15 ml, respectively. The main cultures were carried out in 500 ml Erlenmeyer flasks filled with 100 ml SMG pH 4 inoculated at an OD_{600} of 0.2. Cultures were incubated on an orbital shaker at 30°C, 200 rpm. Samples (1 ml) were taken for OD_{600} measurement and high-performance liquid chromatography (HPLC) analysis at regular intervals.

All experiments for strain characterization in bioreactors were performed in a 2-l bioreactor (BIOSTAT® A plus, Sartorius Stedim Biotech GmbH, Goettingen, Germany) equipped with a Visiferm DO ECS 225 probe for pO_2 measurement (Hamilton Bonaduz AG, Bonaduz, Switzerland). The precultures were prepared using 5 ml of SMD following the aforementioned procedure, while intermediate cultures were prepared in 50 ml of SMG (pH 4). Cells from the intermediate culture were harvested during the exponential growth phase and used to inoculate 1 l of SMG in the bioreactors at an initial OD of 1.0. To support the formation of higher biomass concentrations, the concentrations of vitamins and trace elements were doubled. The culture pH was maintained at 4.0, and the temperature was controlled at 30°C. Dissolved oxygen (DO) levels were maintained above 30% saturation by modulating the air flow rate and stirring speed to avoid oxygen limitation. The cell dry weight was determined at regular intervals using a method adapted from Signori et al. (2016).

Metabolite analysis

Culture samples of 1 ml volume were filtered using a 0.22 µm MiniSart RC membrane filter (Sartorius, Göttingen, Germany) and subjected to HPLC to determine the concentrations of glycerol and ethanol. The Waters HPLC system (Eschborn, Germany) was equipped with an Aminex HPX-87H cation exchange column (Biorad, Munich, Germany) linked to a refractive index (RI) detector (Waters 2412). The column and detector were maintained at 45°C and 30°C, respectively. During the analysis, samples were kept at 15°C and 20 µl aliquots were run for 30 min using 5 mM H_2SO_4 (0.6 ml/min) as mobile phase. Under the described conditions, glycerol and ethanol showed a retention time of ~14 and 21 min, respectively. The data were processed using the Breeze 2 software (Waters). Quantitative analysis was based on standards containing glycerol and ethanol in increasing concentrations (1–100 g/l and 0.3–30 g/l).

Rate and yield calculations

Volumetric and specific glycerol consumption rates were calculated for 1-h time intervals, based on a curve fit to the available data in a way that minimizes the discrepancy between calculated and determined values. Biomass yields were calculated by dividing the biomass formed (in Cmol) by the glycerol consumed up to the respective time point. For shake flask experiments, measured OD_{600} values were converted to cell dry weight (CDW) using a standard curve.

Results

Construction of three isogenic *S. cerevisiae* CEN.PK113-1A derivatives containing the G3P pathway, the DHA pathway, or both for glycerol catabolism

The strain CEN.PK113-1A $UBR2_{CBS}$ $GUT1_{JL1}$ (Supplementary Table S1) was used as the parental strain for constructing the three strains shown in Fig. 1C. The detailed construction history and genetic constitution of the strains are explained in the "Material and Methods" section and shown in Supplementary Fig. S1. In brief, the first step was to equip the strain CEN.PK113-1A $UBR2_{CBS}$ $GUT1_{JL1}$ with a *CjFPS1* expression cassette, resulting in the strain CEN $G3P_{PW}$. In parallel, the isogenic strain CEN TWO_{PW} was constructed by integrating the expression cassettes for *CjFPS1*, *Opgdh*, and *DAK1* into the parental strain. The strain CEN DHA_{PW} was constructed by deleting the *GUT1* gene (more precisely, the $GUT1_{JL1}$ allele) in the strain CEN TWO_{PW}.

Maximum specific growth rates measured in the Growth Profiler

The three constructed strains, CEN $G3P_{PW}$, CEN DHA_{PW}, and CEN TWO_{PW} (Fig. 1C), were first characterized with regard to their μ_{max} in SMG using the Growth Profiler as described in the "Material and Methods" section. The data shown in Fig. 2 reveal that a high μ_{max} around 0.25 h^{-1} was only observed in the strains CEN DHA_{PW} and CEN TWO_{PW}, i.e. when the DHA pathway was present either alone or together with the G3P pathway. The strain CEN $G3P_{PW}$ only showed a μ_{max} of about 0.05 h^{-1}. One has to consider that

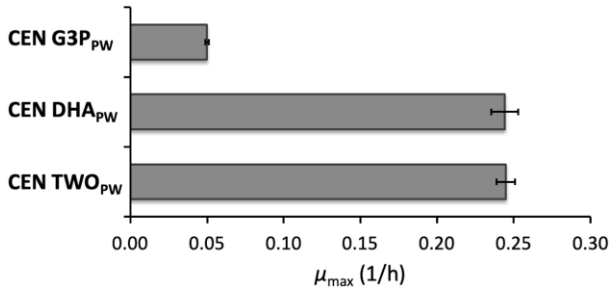

Figure 2. Maximum specific growth rates (μ_{max}) of three isogenic *S. cerevisiae* strains exhibiting different glycerol catabolic pathways. The CEN TWO$_{PW}$ strain contains all genetic modifications leading to (i) an optimized version of the endogenous G3P pathway, (ii) the synthetic NADH-delivering DHA pathway, and (iii) the aquaglyceroporin from *C. jadinii* (*CjFPS1*). The two isogenic control strains both contain *CjFPS1* and the optimized version of the endogenous G3P pathway (CEN G3P$_{PW}$) or the synthetic NADH-delivering DHA pathway (CEN DHA$_{PW}$). The experiments were conducted in synthetic medium with glycerol as the carbon source (SMG) and urea as the nitrogen source (pH 5). The depicted data are average values and standard deviations derived from four biological replicates.

the specific growth rates measured in the Growth Profiler reached their maximum at the very beginning of exponential growth, i.e. when cell densities were low and oxygenation was supposed to be optimal.

Characterization of the strains CEN DHA$_{PW}$ and CEN TWO$_{PW}$ in shake flask cultivations

As a next step, the two fast-growing strains, CEN DHA$_{PW}$ and CEN TWO$_{PW}$, were tested in conventional shake flasks in which oxygen is known to become a growth-limiting factor as soon as higher cell densities are reached. We used 20% filling volume (see Material and Methods) since this condition has been known to cause a switch from respiratory to respiro-fermentative metabolism in our *S. cerevisiae* strains, which exclusively use the DHA pathway for glycerol catabolism (Aßkamp et al. 2019). Indeed, a respective CEN.PK113-1A derivative produced up to about 5 g/l ethanol from glycerol under these conditions (Perpelea et al. 2022). Accordingly, the strain CEN DHA$_{PW}$ constructed in the current study also reached a maximum ethanol titer of 3.6 g/l (Fig. 3A). Interestingly, the ethanol formation of the strain CEN TWO$_{PW}$ was considerably higher; the maximum ethanol titer reached about 19 g/l (Fig. 3A). The maximum ethanol yield was increased more than four-fold (0.468 ± 0.008 in CEN TWO$_{PW}$ versus 0.113 ± 0.006 Cmol$_{ethanol}$/Cmol$_{glycerol}$ in CEN DHA$_{PW}$). The high ethanol production in the strain CEN TWO$_{PW}$ was accompanied by a significantly lower biomass titer (Fig. 3A) and yield (Supplementary Fig. S3) when compared to CEN DHA$_{PW}$. When calculating the biomass yield at the time point where ethanol titers peaked in the shake flask experiments (120 h), the value was 0.329 ± 0.026 Cmol$_{CDW}$/Cmol$_{glycerol}$ for CEN DHA$_{PW}$ and 0.102 ± 0.009 Cmol$_{CDW}$/Cmol$_{glycerol}$ for CEN TWO$_{PW}$.

Notably, the strain CEN TWO$_{PW}$ showed a significantly faster metabolic flux of glycerol utilization, as can be seen by the 2.3-fold higher specific glycerol consumption rate compared to the strain CEN DHA$_{PW}$ (Fig. 3B). The specific glycerol consumption rates for this comparison were taken from the time points when volumetric consumption reached its maximum (Fig. 3B) since we considered these values most reliable. While the strain CEN DHA$_{PW}$ reached 0.083 ± 0.006 $g_{glycerol}/g_{CDW}$ h during the time interval of 43–51 h (a range is given here since each replicate reached its maximum volumetric glycerol consumption rate at a slightly different time point), the value for the TWO$_{PW}$ strain was 0.188 ± 0.003 (between 49 and 52 h).

Another relevant result obtained with the strain CEN TWO$_{PW}$ is the improved ability to deplete the glycerol in the medium toward the end of the batch cultivation. While the strain CEN DHA$_{PW}$ slowed down volumetric substrate consumption when glycerol concentrations dropped below 20 g/l and left ~3 g/l glycerol unconsumed, the strain CEN TWO$_{PW}$ used glycerol in an almost linear manner and completely depleted it (Fig. 3A). Moreover, it seems that the faster biomass accumulation of strain CEN DHA$_{PW}$ is associated with an earlier and faster decrease of the culture pH (Fig. 3A). In both cultures, the initial pH of 4 first increases to neutral values, which is common for "DHA pathway strains" when urea is used as the source of nitrogen in the SMG (Malubhoy et al. 2022). However, while the pH for strain CEN TWO$_{PW}$ decreased slowly after 48 h, the culture pH for CEN DHA$_{PW}$ shows a sudden drop to a value of 3 between 48 and 72 h of cultivation.

Characterization of the strains CEN DHA$_{PW}$ and CEN TWO$_{PW}$ in fully aerated batch cultivations in pH-controlled bioreactors

The strains CEN DHA$_{PW}$ and CEN TWO$_{PW}$ were also characterized in batch cultivations in bioreactors in order to investigate the phenotypes under full oxygenation. The use of bioreactors also allowed us to control the pH throughout the cultivation (pH 4). The glycerol concentration at the beginning was the same as in the previous experiments. First, it must be noted that no detectable amount of ethanol was observed at any time point in the fermentation broth of both strains. Similar to the shake flask experiments, the strain CEN TWO$_{PW}$ consumed the glycerol much faster, and there was no glycerol left at the end of the experiment (Fig. 4A). However, it was surprising that the leftover glycerol for the strain CEN DHA$_{PW}$ (34 g/l) was considerably higher compared to the shake flask experiment.

When compared to the shake flask experiments, the conditions in the bioreactor led to an inverse behavior of the two strains in terms of biomass accumulation. In fact, the strain CEN TWO$_{PW}$ grew faster compared to strain CEN DHA$_{PW}$, but both strains reached a similar final biomass titer (Fig. 4A). Supplementary Fig. S3 shows that the biomass yields for both strains change over time. Moreover, we do not have data for time points before 24 h for the shake flask experiments, which impedes a direct comparison between the two conditions. Still, the conditions in the bioreactor resulted in generally higher biomass yields compared to our shake flask setup. Despite the fact that we cannot exclude that a minor ethanol evaporation might occur for cultivation with strain CEN TWO$_{PW}$, it seems unlikely that this can justify the difference in biomass yield. It is important to note that the biomass yields of the two strains in the bioreactor experiment resemble each other at two early time points: 12 and 16 h. Only afterward, the strain CEN TWO$_{PW}$ showed a significantly lower biomass yield compared to strain CEN DHA$_{PW}$. So far, we do not have an explanation for these results.

We were also interested in whether the strain CEN TWO$_{PW}$ also exhibits a higher metabolic flux of glycerol utilization under the controlled conditions in the bioreactor. Therefore, we plotted

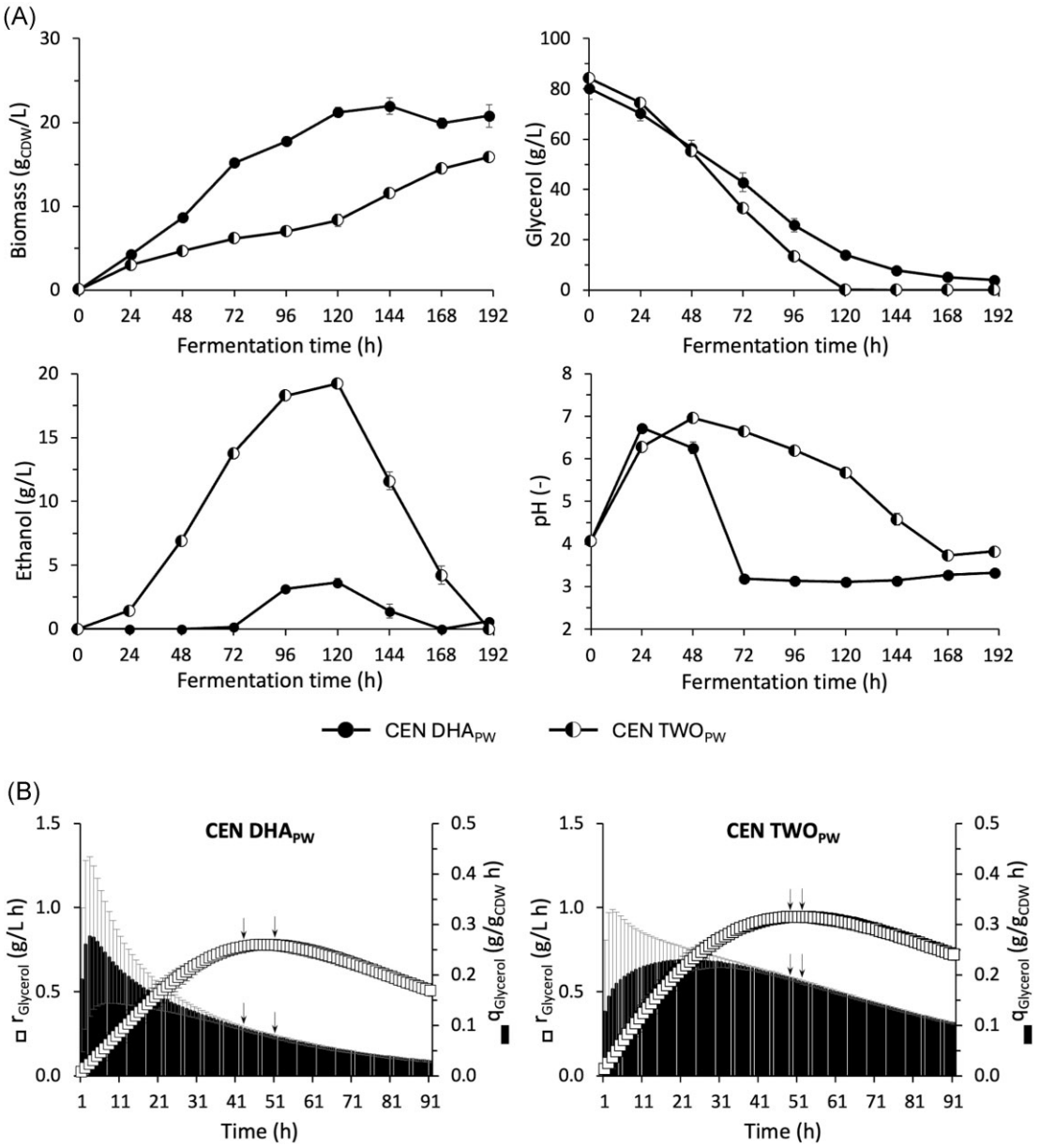

Figure 3. (A) Fermentation profile comparison between CEN DHA_{PW} and CEN TWO_{PW}. Strains are represented as filled symbols (CEN DHA_{PW}) and half-filled for CEN TWO_{PW}. Batch cultivation was performed in 500 ml Erlenmeyer flasks filled at 20% of capacity with SMG with urea at initial pH 4. Cultures were inoculated, adjusting an OD_{600} of 0.2 (corresponding to approximately 0.09 g_{CDW}/l). Average values and standard deviations are derived from biological triplicates. (B) Specific (black bars) and volumetric (white squares) glycerol consumption rates for CEN DHA_{PW} and CEN TWO_{PW} in the first 91 h of cultivation. The arrows indicate the time interval where the maximum volumetric consumption rate was achieved for each of the three biological replicates.

the calculated values for the specific glycerol consumption rates over time for both strains (Fig. 4B). The values for the volumetric consumption rates were also included in the figure. Although we treat the absolute values with care (due to the low number of actual data points and the measurement uncertainties at high glycerol concentrations), the results reveal again a clear difference between the two strains, confirming a significantly (roughly 1.6-fold) faster flux of glycerol consumption in strain CEN TWO_{PW} compared to strain CEN DHA_{PW}. When we consider again the values for the specific rates at the time points when the volumetric rates reached their maximum, we obtain 0.159 (±0.01) and 0.252 (±0.01) $g_{glycerol}/g_{CDW}$ h for the DHA_{PW} and TWO_{PW} strains, respectively.

The abolishment of the G3P pathway by deletion of *GUT2* in the strain CEN TWO_{PW} resulted in a different phenotype compared to the deletion of *GUT1*

The question arose whether the remarkable phenotype of strain CEN TWO_{PW} (faster glycerol consumption and higher ethanol yield in shake flask experiments) can be attributed to the additional carbon flux via the G3P pathway. Therefore, we tested whether the deletion of *GUT2* in the CEN TWO_{PW} background results in a similar phenotype as observed for the strain CEN DHA_{PW}. Gut2p catalyzes the second step within the G3P pathway (Fig. 1). We constructed the respective strain by deleting *GUT2* in strain CEN TWO_{PW}, resulting in strain CEN TWO_{PW} *gut2*Δ

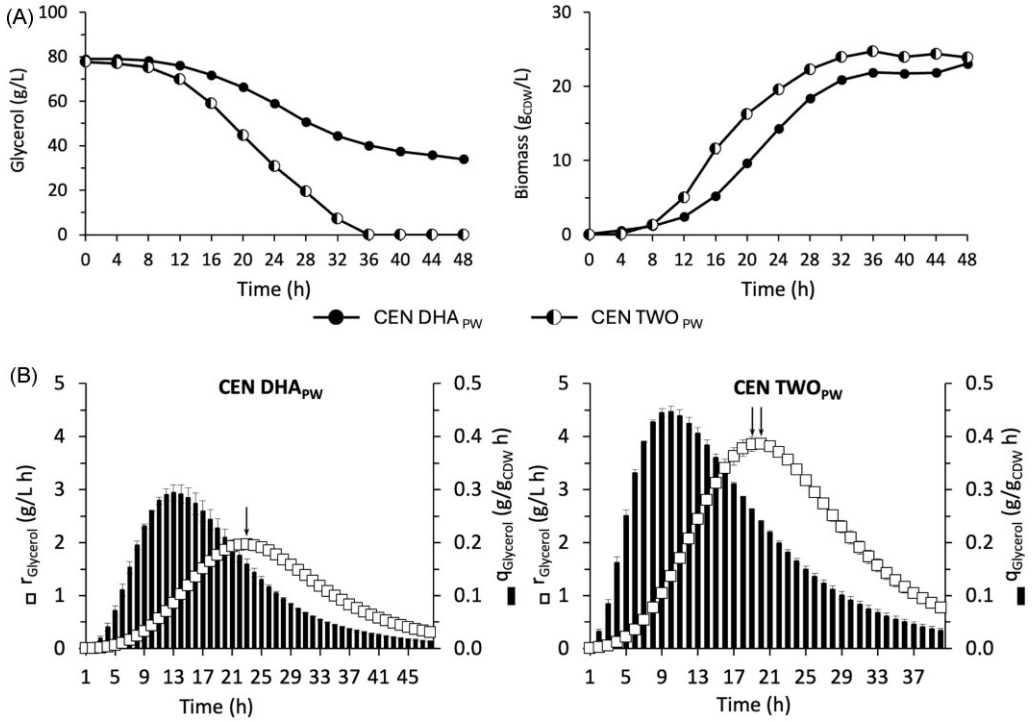

Figure 4. (A) Glycerol consumption and biomass production for the strains CEN DHA$_{PW}$ and CEN TWO$_{PW}$ in aerobic, pH-controlled (pH 4.0) bioreactor cultivations. Average values and absolute deviations are derived from biological duplicates. Absolute deviations for biomass and glycerol measurements were too small to be visible over the symbols. (B) Volumetric (white squares) and specific (black bars) glycerol consumption rates determined for 1-h intervals. The arrows indicate the time point(s) where the maximum volumetric glycerol consumption rate was reached.

(Supplementary Fig. S4), i.e. another derivative whose glycerol catabolism solely relies on the DHA pathway. However, it is important to note that unlike deleting *GUT1* (strictly speaking, the mutant allele *GUT1*$_{JL1}$), which completely prevents glycerol from entering the G3P pathway, deleting *GUT2* still allows glycerol phosphorylation to G3P (via the mutant allele *GUT1*$_{JL1}$) at the expense of ATP. Therefore, the metabolic impact of *GUT2* deletion may not mirror that of *GUT1* deletion. However, deleting *GUT2* is supposed to also disable any flux of carbon from glycerol via the G3P pathway into glycolysis. We tested the performance of this strain under oxygen-limited conditions in shake flasks (Fig. 5). The strains CEN TWO$_{PW}$ (*GUT1*$_{JL1}$; *GUT2*) and CEN DHA$_{PW}$ (*gut1*$_{JL1}$Δ; *GUT2*) served as controls in this experiment.

Similar to the strain CEN DHA$_{PW}$ (*gut1*$_{JL1}$Δ; *GUT2*), the isogenic strain CEN DHA$_{PW}$ (*GUT1*$_{JL1}$; *gut2*Δ) did also not show the high glycolytic flux/ethanol production that could only be observed when both pathways were present in CEN TWO$_{PW}$ (*GUT1*$_{JL1}$, *GUT2*). However, the behavior of CEN DHA$_{PW}$ (*GUT1*$_{JL1}$; *gut2*Δ) did not fully match that of strain CEN DHA$_{PW}$ (*gut1*$_{JL1}$Δ; *GUT2*). In fact, the kinetics of biomass formation differed significantly. The *gut2*Δ deletion strain rather resembled strain CEN TWO$_{PW}$ in this context. It might be that the latter strain formed a by-product that was directly co-used for biomass production, but we do not have any proof for this assumption.

The difference between the phenotypes of the strain CEN TWO$_{PW}$ and CEN DHA$_{PW}$ seems to be attributed to the particular point mutation in the *GUT1*$_{JL1}$ allele

It is important to highlight that the only difference between the strain CEN TWO$_{PW}$ and CEN DHA$_{PW}$ (*gut1*$_{JL1}$Δ; *GUT2*) is the deleted *GUT1*$_{JL1}$ in the latter strain as shown in Fig. 1C. This brought us to the hypothesis that the presence of an active glycerol kinase might have contributed to the phenotype of CEN TWO$_{PW}$. While the results obtained with the isogenic strain CEN DHA$_{PW}$ (*GUT1*$_{JL1}$; *gut2*Δ) suggest that a fully functional G3P pathway (i.e. Gut1 and Gut2 both functional) is required for the phenotype observed in strain CEN TWO$_{PW}$, it did not clarify the specific role of *GUT1*$_{Jl1}$. We further speculated that the particular mutant allele of *GUT1* (*GUT1*$_{Jl1}$), which is present in the strain CEN TWO$_{PW}$, could influence not only the glycerol kinase activity but also potentially modify any potential regulatory functions of the enzyme. Notably, the *GUT1*$_{JL1}$ allele present in the strain CEN TWO$_{PW}$ is a mutant allele originating from the strain JL1, a strain previously obtained by ALE (Ochoa-Estopier et al. 2011) and elucidated by Ho et al. (2017). In fact, *GUT1*$_{JL1}$ contains a single amino acid exchange in comparison to the CEN.PK wild-type enzyme (Ser118Phe).

As described in the introduction, our laboratory also identified *GUT1*$_{CBS}$ as a superior allele of *GUT1*. In fact, the *GUT1*$_{CBS}$ allele was also able to allow growth rates up to 0.13 h^{-1} when combined with a superior *UBR2* allele (Swinnen et al. 2016, Ho et al. 2017). The availability of the two different superior *GUT1* alleles having different single-point mutations prompted us to compare both alleles in the CEN TWO$_{PW}$ strain scenario. For this purpose, we replaced the *GUT1*$_{JL1}$ allele with the *GUT1* allele from CBS 6412-13A (*GUT1*$_{CBS}$). We also constructed an isogenic strain that contains the wild-type *GUT1* allele (*GUT1*$_{CEN}$) from the strain CEN.PK113-1A. Supplementary Fig. S2 shows how the *GUT1* alleles differ in their deduced amino acid sequence. To our surprise, the "TWO pathway strain" (*GUT1*; *GUT2*) with the *GUT1*$_{CBS}$ allele did not behave at all as our above-described strain CEN TWO$_{PW}$ containing the *GUT1*$_{JL1}$ allele (Fig. 6). Despite showing similar glycerol consumption patterns, the other three physiological parameters, such as the kinetics of biomass and ethanol formation as well as

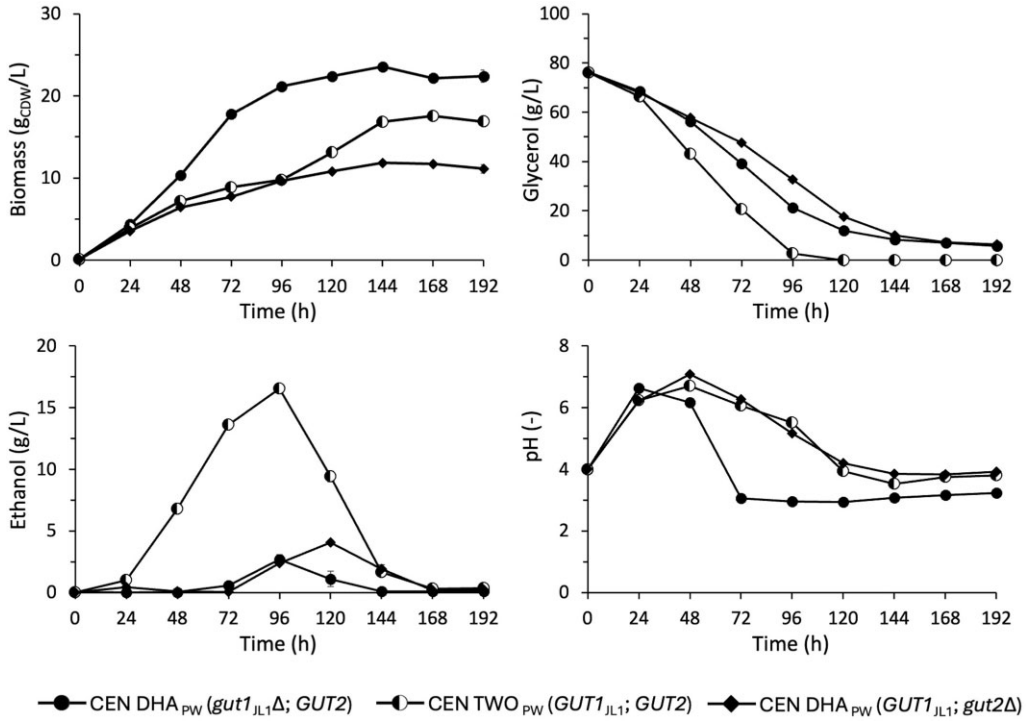

Figure 5. Shake flask fermentative profile comparison between CEN TWO_{PW}, CEN DHA_{PW} (*gut1*Δ), and CEN DHA_{PW} (*gut2*Δ). The three analyzed strains all carried a functional DHA pathway but differed with regard to the G3P pathway: (i) fully functional G3P pathway (TWO_{PW} strain = $GUT1_{JL1}$; *GUT2*), (ii) inactive G3P pathway by deletion of *GUT1* (CEN DHA_{PW} = $gut1_{JL1}$Δ; *GUT2*), and (iii) inactive G3P pathway by deletion of *GUT2* (CEN DHA_{PW} = $GUT1_{JL1}$; *gut2*Δ). Average values and standard deviations are derived from biological triplicates.

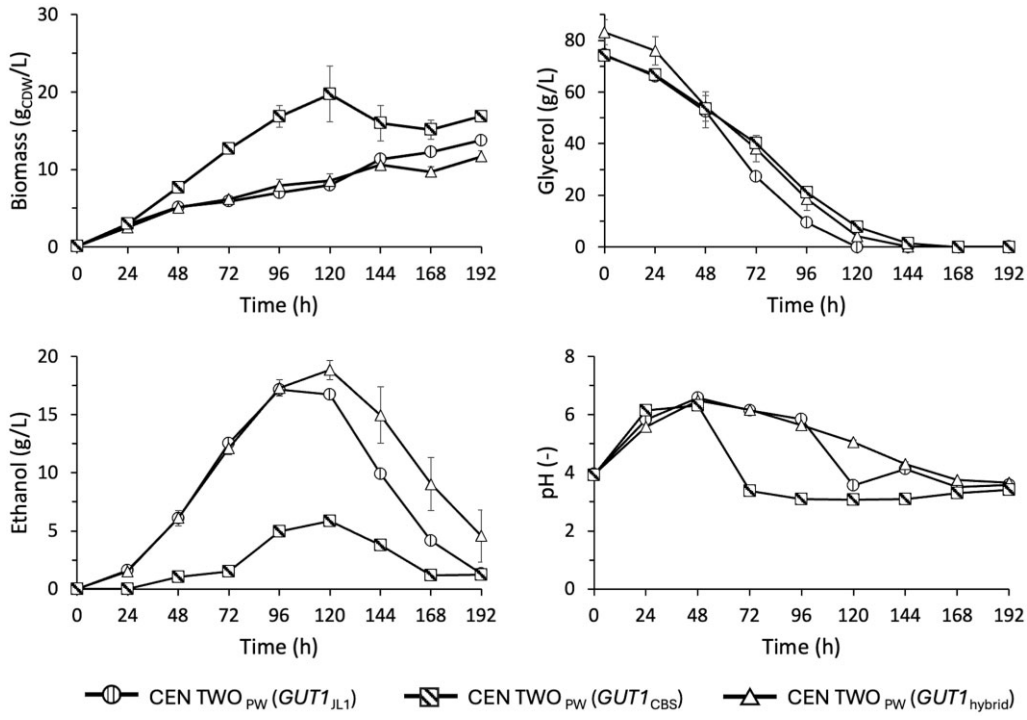

Figure 6. Shake flask fermentative profile comparison between CEN TWO_{PW} ($GUT1_{JL1\ allele}$), CEN TWO_{PW} ($GUT1_{CBS\ allele}$), and CEN TWO_{PW} ($GUT1_{hybrid\ allele}$). Average values and standard deviations are derived from biological triplicates. Data for CEN TWO_{PW} ($GUT1_{CEN\ wild\text{-}type\ allele}$) are not shown; the strain exhibits the same phenotype as the strain CEN TWO_{PW} ($GUT1_{CBS\ allele}$).

of pH, differed. In fact, its behavior resembled that of the strain CEN DHA_{PW} (*gut1*Δ; *GUT2*) (compare to Fig. 3A) and the strain CEN TWO_{PW}, which carried the $GUT1_{CEN}$ allele (data not shown). The results suggested that particularly the different amino acid at position 118 (phenylalanine in $GUT1_{JL1}$ and serine in $GUT1_{CBS}$) has a major impact on the phenotype.

To further substantiate our hypothesis, we also created a strain carrying a hybrid variant of the two alleles by introducing the single point mutation from the $GUT1_{JL1}$ allele into the $GUT1_{CBS}$ allele, leading to the replacement of serine at position 118 by phenylalanine (Supplementary Fig. S2). The CEN TWO_{PW} derivative carrying the resulting $GUT1_{hybrid}$ allele showed the same phenotype as the isogenic derivative carrying the $GUT1_{JL1}$ allele (Fig. 6). This result provides strong evidence that the amino acid exchange at position 118 of the Gut1 of JL1 plays a pivotal role in the phenotypic characteristics of the CEN TWO_{PW} strain.

Discussion

As described in the introduction, our group engineered *S. cerevisiae* for glycerol utilization by either modifying the endogenous FAD-dependent G3P pathway or by implementing the synthetic NAD-dependent DHA pathway. One major motivation for establishing glycerol utilization in the popular yeast cell factory *S. cerevisiae* was the fact that glycerol can deliver more electrons per carbon compared to sugars in the biotechnological production of small molecules from glycerol, such as 1,2-propanediol (Islam et al. 2017) and succinic acid (SA) (Xiberras et al. 2020, Malubhoy et al. 2022, Rendulić et al. 2024). In all these applications of glycerol-utilizing *S. cerevisiae* strains, we exclusively used the NADH-delivering "DHA pathway" and abolished the endogenous G3P pathway by *GUT1* deletion. The current study has been mainly motivated by the question of whether the existence of the endogenous G3P pathway provides advantages for glycerol utilization when it is present in parallel to our synthetic DHA pathway.

The construction of the strain carrying the two glycerol utilization pathways (CEN TWO_{PW}) was guided by our state-of-the-art knowledge on how to individually optimize each pathway in the genetic background of the strain CEN.PK113-1A. The two, otherwise isogenic, control strains (CEN $G3P_{PW}$ and CEN DHA_{PW}) were constructed here in a way to be isogenic to the strain CEN TWO_{PW} in any aspect apart from the metabolic route(s) from intracellular glycerol to DHAP. Before discussing the results in detail, we want to highlight that the results obtained in the current study might be specific for the CEN.PK background and probably cannot be generalized.

The construction of the strain CEN $G3P_{PW}$ allowed us to conclude that the presence of *CjFPS1* did not improve the μ_{max} of the baseline strain CEN.PK113-1A $UBR2_{CBS}$ $GUT1_{JL1}$, which did not have a heterologous glycerol transporter. This result suggests that the low maximum growth rate of the baseline strain explicitly using the G3P pathway was not caused by a suboptimal import of glycerol due to the lack of *CjFPS1* expression. It was not in the scope of the current study to further improve the flux in the strain CEN $G3P_{PW}$.

While the maximum specific growth rate of the strain CEN $G3P_{PW}$ was around 0.050 h^{-1}, the values for the strains CEN DHA_{PW} and CEN TWO_{PW} were about 5 times higher, i.e. 0.244 h^{-1} and 0.245 h^{-1}. These results reveal that the additional presence of our G3P pathway did not provide a significant advantage for the maximum rate of biomass formation under optimal growth conditions (i.e. aerobic and low cell density). It seems that the maximal growth rate under these conditions is limited by metabolic reactions other than the conversion of glycerol to DHAP, such as the downstream metabolic network, or by thermodynamic constraints (Niebel et al. 2019). In general, it would be interesting to know the carbon flux distributions between the two pathways and whether there is flux through the G3P pathway at all under the conditions that allow maximum growth rate. However, to the best of our knowledge, there is no method available to quantify these two parallel fluxes from glycerol to DHAP. Based on the data obtained, we cannot exclude that the presence of the glycerol kinase variant from JL1 in the CEN TWO_{PW} increased the flux through the DHA pathway and glycolysis, but not the flux through the G3P pathway (see below). Despite their similar μ_{max} in the Growth Profiler (Fig. 2), the two fast-growing strains, CEN DHA_{PW} and CEN TWO_{PW}, exhibited strikingly different phenotypes when their physiology was studied over time in batch cultivations.

The fact that strains exhibiting the synthetic DHA pathway switch to fermentation in shake flasks has already been observed in the past and assumed to be caused by an overflow metabolism due to the excess of cytosolic NADH during oxygen limitation at higher cell densities (Aßkamp et al. 2019, Xiberras et al. 2020, Perpelea et al. 2022). We originally assumed that the phenotype of the strain CEN TWO_{PW} would resemble that of strain CEN DHA_{PW} in the oxygen-limited shake flask experiments. In fact, the G3P pathway does not result in NADH formation on the way from glycerol to DHAP. Instead, the activity of Gut2 (catalyzing the second step of the G3P pathway) depends on the oxidation of enzyme-bound $FADH_2$ by the respiratory chain. Therefore, we expected that the latter would become a bottleneck when oxygen supply is limited. However, the strain CEN TWO_{PW} showed a generally faster glycolytic flux (postulated based on the higher specific glycerol consumption rate), a by far higher overflow metabolism to ethanol, and produced less biomass in the shake flasks compared to the strain CEN DHA_{PW}.

Notably, the only difference between the strain CEN TWO_{PW} and the strain CEN DHA_{PW} is a lack of glycerol kinase activity in the latter, caused by a deletion of $GUT1_{JL1}$. The latter is the only allele of *GUT1* present in the strain CEN TWO_{PW} and represents a mutated allele. Based on our results, it seems that, for the fast glycerol consumption and the strong overflow metabolism of the strain CEN TWO_{PW} in the shake flasks, at least the following prerequisites have to be present: (i) the DHA pathway and (ii) the optimized G3P pathway based on the JL1-specific mutation in the used *GUT1* allele.

The single point mutation in the *GUT1* allele originating from the evolved strain JL1 clearly contributes to the phenotype of our CEN TWO_{PW} strain. This conclusion is based on the following facts: (i) The replacement of $GUT1_{JL1}$ with $GUT1_{CBS}$ in an otherwise isogenic background resulted in a phenotype similar to CEN DHA_{PW} (Fig. 3A, Fig. 6), which does not have any *GUT1* gene in its genome, and (ii) the introduction of the JL1 mutation into the allele from $GUT1_{CBS}$ in the first strain restored the fast glycerol consumption and high ethanol production characteristic of CEN TWO_{PW}. We attempted to measure the *in vitro* glycerol kinase activities in crude extracts of the constructed isogenic strains with the different *GUT1*. However, the standard assay previously used by others (Hayashi and Lin 1967, Ho et al. 2017) resulted in a high background activity in an isogenic *gut1* deletion mutant. We assume that the presence of the synthetic DHA pathway in this strain and those carrying the different *GUT1* alleles complicated the data interpretation since the DHA pathway involves high cellular activities of glycerol dehydrogenase and DHA kinase. This

pathway also consumes glycerol and can produce NADH as well as consume ATP, the same substrate/cofactors used in the standard glycerol kinase assay (Hayashi and Lin 1967, Ho et al. 2017). Apart from the high background activity, we did not find any correlation between the measured activity and the strain's phenotype (data not shown). Nevertheless, we would like to emphasize that *in vitro* enzyme measurements generally do not provide sufficient information about the actual *in vivo* activity. It might well be that the mutation results in a different *in vivo* flux due to a different regulation by intracellular metabolites. It can also not be excluded that the glycerol kinase from *S. cerevisiae* has more functions in the cell than solely converting glycerol into L-G3P. Several studies conducted in bacteria or in human cells have already demonstrated that mutant versions of glycerol kinase cause pleiotropic effects (Yeh et al. 2009, Sriram et al. 2010). It will be the scope of future research to understand the impact of the mutation at the molecular level.

An interesting observation when comparing the strains CEN TWO_{PW} and CEN DHA_{PW} was the decelerated volumetric glycerol consumption of the latter strain toward the end of the cultivation and that growth ceased well before glycerol in the culture medium was depleted. We already realized this behavior of "DHA pathway strains" in bioreactor experiments conducted in previous studies, but the final glycerol concentration was much lower (Xiberras et al. 2020, Malubhoy et al. 2022). It must be mentioned that the strains analyzed in these two studies have been equipped with a pathway for SA production (i.e. a strong sink for NADH). This is a major difference from the current study. An incomplete glycerol utilization by the strain CEN DHA_{PW} was also visible in the shake flask experiments conducted in our current work, even though the final glycerol concentration was relatively low. This behavior of "DHA pathway strains" could have been caused by the kinetic properties of the first enzyme of the DHA pathway (the glycerol dehydrogenase from *O. parapolymorpha*—Opgdh) catalyzing the NAD^+-dependent oxidation of glycerol to DHA. Yamada-Onodera et al. (2002) reported K_m values (*in vitro*) of 118 mM for glycerol and of 4.87 µM for DHA. Moreover, the pH optimum for glycerol oxidation was determined to be 10. This data indicates that intracellular glycerol concentration must be relatively high to allow sufficient *in vivo* flux through Opgdh. Decreasing glycerol concentrations in the medium toward the end of the cultivation may result in decreased glycerol influx. Consequently, glycerol oxidation may become the rate-controlling step in glycerol catabolism, particularly when the pull by the downstream flux is not strong enough.

However, the question remains why the downstream metabolic pull is much higher in the strain CEN TWO_{PW} compared to CEN DHA_{PW}. This question is indeed difficult to answer. In previous studies we observed that the glycolytic flux in strains (exclusively) using the DHA pathway for glycerol catabolism was significantly increased when a pathway toward the production of SA was established (Malubhoy et al. 2022, Rendulić et al. 2024). We concluded that the engineered NADH-consuming SA pathway (reductive TCA pathway) resulted in a very strong pull toward the target product, causing an increased glycolytic flux (visible by an increased specific glycerol consumption rate). The data presented in the current study show that the establishment of the G3P pathway based on $Gut1_{JL1}$ also increased the glycolytic flux even without the SA production pathway. So far, we lack sufficient data to understand the regulatory function of $Gut1_{JL1}$ on central carbon metabolism and the particular consequences of exchanging the single amino acid at position 118 (Ser118Phe). Serine is the amino acid residue in proteins most commonly phosphorylated (Schwartz and Murray 2011). We speculated that the serine in the *GUT1* wild-type allele in CEN.PK113-1A and the allele isolated from CBS 6412-13A could be a phosphorylation site that was removed in the JL1 allele. However, according to the information provided by UniProt, this amino acid position in Gut1 does not belong to the known binding sites for glycerol or ATP.

Conclusions

Although the molecular basis for the results obtained here with the strain CEN TWO_{PW} are not yet completely clear, it can be concluded that this strain has several attractive features for *S. cerevisiae*-based bioprocesses applying glycerol as a substrate. The fast glycerol consumption rate is certainly an asset in all types of processes. The strain showed the highest growth rate of all strains under full aeration, which is particularly relevant for the production of growth-associated products such as proteins or for biomass production per se. Under oxygen-limited conditions, the strain can switch to fermentation, which is attractive for the production of reduced small molecules. Notably, the strain seems to offer itself as a system to decouple growth and product formation since a limitation of oxygen could switch from biomass formation to fermentation or biotransformation. Apart from its biotechnological relevance, the presented data suggests the existence of regulatory mechanisms in central carbon metabolism caused by glycerol kinase that have been uncovered so far.

Supplementary data

Supplementary data is available at *FEMSYR Journal* online.

Conflict of interest: None declared.

Funding

This work was supported by the European Union's Horizon 2020 research and innovation program under the Marie Skłodowska-Curie grant agreement (764 927) and by the German Research Foundation (NE 697/7-1).

References

Aßkamp MR, Klein M, Nevoigt E. *Saccharomyces cerevisiae* exhibiting a modified route for uptake and catabolism of glycerol forms significant amounts of ethanol from this carbon source considered as "non-fermentable". *Biotechnol Biofuels* 2019;**12**:257.

Bai Flagfeldt D, Siewers V, Huang L *et al.* Characterization of chromosomal integration sites for heterologous gene expression in *Saccharomyces cerevisiae*. *Yeast* 2009;**26**:545–51.

Clomburg JM, Gonzalez R. Anaerobic fermentation of glycerol: a platform for renewable fuels and chemicals. *Trends in Biotechnology* 2013;**31**:20–28.

Ferreira C, van Voorst F, Martins A *et al.* A member of the sugar transporter family, Stl1p is the glycerol/H^+ symporter in *Saccharomyces cerevisiae*. *MBoC* 2005;**16**:2068–76.

Finley D, Ulrich HD, Sommer T *et al.* The ubiquitin–proteasome system of *Saccharomyces cerevisiae*. *Genetics* 2012;**192**:319–60.

Gibson DG, Young L, Chuang R-Y *et al.* Enzymatic assembly of DNA molecules up to several hundred kilobases. *Nat Methods* 2009;**6**:343–5.

Gietz RD, Schiestl RH. High-efficiency yeast transformation using the LiAc/SS carrier DNA/PEG method. *Nat Protoc* 2007;**2**:31–34.

Hayashi S-I, Lin ECC. Purification and properties of glycerol kinase from *Escherichia coli*. *Journal of Biological Chemistry* 1967;**242**:1030–5.

Ho P-W, Klein M, Futschik M *et al.* Glycerol positive promoters for tailored metabolic engineering of the yeast *Saccharomyces cerevisiae*. *FEMS Yeast Res* 2018;**18**:19.

Ho P-W, Swinnen S, Duitama J *et al.* The sole introduction of two single-point mutations establishes glycerol utilization in *Saccharomyces cerevisiae* CEN.PK derivatives. *Biotechnol Biofuels* 2017;**10**:10.

Hoffman CS, Winston F. A ten-minute DNA preparation from yeast efficiently releases autonomous plasmids for transformation of *Escherichia coli*. *Gene* 1987;**57**:267–72.

Hu P, Chakraborty S, Kumar A *et al.* Integrated bioprocess for conversion of gaseous substrates to liquids. *Proc Natl Acad Sci USA* 2016;**113**:3773–8.

Islam Z, Klein M, Aßkamp MR *et al.* A modular metabolic engineering approach for the production of 1,2-propanediol from glycerol by *Saccharomyces cerevisiae*. *Metabolic Engineering* 2017;**44**:223–35.

Klein M, Carrillo M, Xiberras J *et al.* Towards the exploitation of glycerol's high reducing power in *Saccharomyces cerevisiae*-based bioprocesses. *Metabolic Engineering* 2016;**38**:464–72.

Klein M, Islam Z, Knudsen PB *et al.* The expression of glycerol facilitators from various yeast species improves growth on glycerol of *Saccharomyces cerevisiae*. *Metabolic Engineering Communications* 2016;**3**:252–7.

Kurtzman CP, Fell JW, Boekhout T. *The Yeasts: A Taxonomic Study*, **Vol. 1**. Amsterdam: Elsevier, 2011.

Malubhoy Z, Bahia FM, de Valk SC *et al.* Carbon dioxide fixation via production of succinic acid from glycerol in engineered *Saccharomyces cerevisiae*. *Microb Cell Fact* 2022;**21**:102.

Naito Y, Hino K, Bono H *et al.* CRISPRdirect: software for designing CRISPR/Cas guide RNA with reduced off-target sites. *Bioinformatics* 2015;**31**:1120–3.

Niebel B, Leupold S, Heinemann M. An upper limit on gibbs energy dissipation governs cellular metabolism. *Nat Metab* 2019;**1**:125–32.

Ochoa-Estopier A, Lesage J, Gorret N *et al.* Kinetic analysis of a *Saccharomyces cerevisiae* strain adapted for improved growth on glycerol: implications for the development of yeast bioprocesses on glycerol. *Bioresource Technology* 2011;**102**:1521–7.

Pavlik P, Simon M, Schuster T *et al.* The glycerol kinase (*GUT1*) gene of *Saccharomyces cerevisiae*: cloning and characterization. *Curr Genet* 1993;**24**:21–25.

Perpelea A, Wijaya AW, Martins LC *et al.* Towards valorization of pectin-rich agro-industrial residues: engineering of *Saccharomyces cerevisiae* for co-fermentation of D-galacturonic acid and glycerol. *Metabolic Engineering* 2022;**69**:1–14.

Rendulić T, Perpelea A, Ortiz JPR *et al.* Mitochondrial membrane transporters as attractive targets for the fermentative production of succinic acid from glycerol in *Saccharomyces cerevisiae*. *FEMS Yeast Res* 2024;**24**:foae009. https://doi.org/10.1093/femsyr/foae009.

Rønnow B, Kielland-Brandt MC. *GUT2*, a gene for mitochondrial glycerol 3-phosphate dehydrogenase of *Saccharomyces cerevisiae*. *Yeast* 1993;**9**:1121–30.

Russmayer H, Egermeier M, Kalemasi D *et al.* Spotlight on biodiversity of microbial cell factories for glycerol conversion. *Biotechnology Advances* 2019;**37**:107395.

Schwartz PA, Murray BW. Protein kinase biochemistry and drug discovery. *Bioorg Chem* 2011;**39**:192–210.

Signori L, Ami D, Posteri R *et al.* Assessing an effective feeding strategy to optimize crude glycerol utilization as sustainable carbon source for lipid accumulation in oleaginous yeasts. *Microb Cell Fact* 2016;**15**:1–19.

Sprague GF, Cronan JE. Isolation and characterization of *Saccharomyces cerevisiae* mutants defective in glycerol catabolism. *J Bacteriol* 1977;**129**:1335–42.

Sriram G, Parr LS, Rahib L *et al.* Moonlighting function of glycerol kinase causes systems-level changes in rat hepatoma cells. *Metabolic Engineering* 2010;**12**:332–40.

Steiger MG, Mattanovich D, Sauer M. Microbial organic acid production as carbon dioxide sink. *FEMS Microbiol Lett* 2017;**364**:fnx212. https://doi.org/10.1093/femsle/fnx212.

Swinnen S, Ho P-W, Klein M *et al.* Genetic determinants for enhanced glycerol growth of *Saccharomyces cerevisiae*. *Metabolic Engineering* 2016;**36**:68–79.

Swinnen S, Klein M, Carrillo M *et al.* Re-evaluation of glycerol utilization in *Saccharomyces cerevisiae*: characterization of an isolate that grows on glycerol without supporting supplements. *Biotechnol Biofuels* 2013;**6**:157.

Takors R, Kopf M, Mampel J *et al.* Using gas mixtures of CO, CO_2 and H_2 as microbial substrates: the do's and don'ts of successful technology transfer from laboratory to production scale. *Microbial Biotechnology* 2018;**11**:606–25.

Verduyn C, Postma E, Scheffers WA *et al.* Effect of benzoic acid on metabolic fluxes in yeasts: a continuous-culture study on the regulation of respiration and alcoholic fermentation. *Yeast* 1992;**8**:501–17.

Xiberras J, Klein M, de Hulster E *et al.* Engineering *Saccharomyces cerevisiae* for succinic acid production from glycerol and carbon dioxide. *Front Bioeng Biotechnol* 2020;**8**:566. https://doi.org/10.3389/fbioe.2020.00566.

Yamada-Onodera K, Yamamoto H, Emoto E *et al.* Characterisation of glycerol dehydrogenase from a methylotrophic yeast, *Hansenula polymorpha* dl-1, and its gene cloning. *Acta Biotechnol* 2002;**22**:337–53.

Yang F, Hanna MA, Sun R. Value-added uses for crude glycerol-a byproduct of biodiesel production. *Biotechnol Biofuels* 2012;**5**:13.

Yeh JI, Kettering R, Saxl R *et al.* Structural characterizations of glycerol kinase: unraveling phosphorylation-induced long-range activation. *Biochemistry* 2009;**48**:346–56.

Received 29 August 2024; **revised** 4 March 2025; **accepted** 28 March 2025